PARTIAL DISCHARGE (PD) SNIFFER FOR WORKERS' SAFETY IN UNDERGROUND VAULTS

François LÉONARD
Hydro-Québec – Canada
leonard.frnacois@ireq.ca

Lionel REYNAUD
Hydro-Québec – Canada
reynaud.lionel@ireq.ca

Jacques BHERER
Hydro-Québec – Canada
bherer.jacques@ireq.ca

Daniel PINEAU
Hydro-Québec – Canada
pineau.daniel@ireq.ca

Didier MUSSARD
Hydro-Québec – Canada
mussard.didier@ireq.ca

Sylvain POIRIER
Hydro-Québec – Canada
poirier.sylvain@ireq.ca

Stéphane GINGRAS
Hydro-Québec – Canada
gingras.stephane@ireq.ca

ABSTRACT

In 15 seconds, many hundred transitory electromagnetic events are captured and analyzed before flashing the LED that informs the worker about PDs indicating a dangerous failure mode. Many new ideas have been put forward to explain this performance. Some are found in the hardware but the most important are in signal processing: time domain clustering (TDC) and phase-resolved partial discharge (PRPD) data mining (PD mining). This paper exposes these new ideas and shows some results collected in the field.

INTRODUCTION

Since 2006, the Hydro-Québec Partial Discharge Analyzer (PDA) [1] has been widely used by workers, for safety reasons, to perform preventive maintenance and to remove defective components prior to their failure. Diagnosis with the PDA is not fully automatic and requires that a final decision be made by an expert. Moreover, the overall time from setup to diagnosis is a safety concern when a worker remains inside the vault. In 2009, Hydro-Québec deployed a PD sniffer capable of delivering an automated diagnosis in under 15 seconds. This new tool is used by non-expert workers for their own safety. When a potential PD is detected by the equipment, the worker exits the vault and calls the PDA/thermograph team. The sniffer captures the transitory events at a rate of 1 Gs/s, groups similar time shape signals across many hundreds of events into clusters, analyzes the resulting clusters' signatures in a "relative phase-resolved" diagram, identifies clusters having inverse polarities and concludes on the potential presence of a PD. Grouping into clusters dramatically reduces the processing time and significantly increases the signal-to-noise ratio. This allows the trigger level to be set so as to capture a PD close to the noise level or below some other PD activity levels with the help of the PD mining.

HARWARE DESCRIPTION

The PD sniffer head (Fig.1) includes a PD reception antenna, a magnetic sensor for phase-resolved synchronization and an emission antenna for self-testing. Shown in Figure 2, the PD antenna has a 350-MHz band-width connected to a hi-pass filter. The controller selects the filter block for the antenna signal, selects the gain value, fixes the trigger level, and enables the trigger when the expected phase value is reached. In the PD sniffer, the trigger enable is synchronized with the line phase. At the trigger enabling, the maximum number of captured segments is fixed with a maximum observation time duration. The trigger is active on the higher gain channel. When an FM signal is disturbing the measurement, the controller enables an external trigger connected to the antenna through an FM notch filter (100 MHz). The signal numerical conversion is done at 1 Gs/s in tandem using the two available channels on two 8-bit scales. This parallel conversion accelerates the measurement process and increases to 12 bits the effective input dynamic. The emission antenna allows the testing of the hardware and software chain (not shown in Fig. 2).

Fig. 1 Sniffer probe.

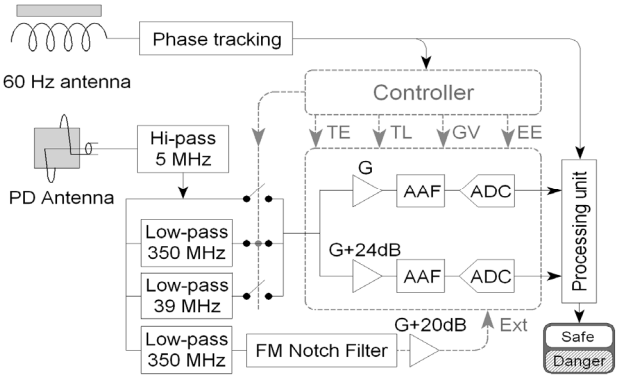

Fig. 2 Sniffer hardware: trigger enable (TE), trigger level (TL), gain value (GV), external trigger enable (EE), external trigger input (Ext), anti-aliasing filter (AAF).

SIGNAL PROCESSING AND DIAGNOSTIC

Many authors [2-5] propose a clustering based on the information available in a multidimensional PRPD distribution and other features such as autocorrelation coefficients [6] or principal component analysis coefficients [7], for example. Based on the field survey, multidimensional PRPD does not discriminate all the clusters: automated diagnosis is not possible and manual

diagnosis is not facilitated by the mixed clusters. Moreover, autocorrelation and the power spectrum process wipe the signal phase information, including the polarity information. Note that the Fourier transform phase contains barely 50% of the information about the time transient pattern. The proposed time domain clustering (TDC) is a process close to the maximum likelihood preserving both amplitude and phase. The next chapter details the TDC algorithm. When the external trigger is enabled, a numerical FM filter may be applied before interpolation. The TDC follows the interpolation as illustrated in Figure 3. A few hundred time samples describe the transient pattern. Segment capture is done on different scales. During the segment capture on a scale, the TDC processes the previous scale captures: PD capture and TDC are parallel processes except at the end where a TDC is done to merge all scales.

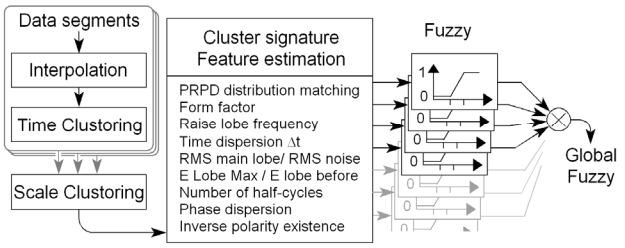

Fig. 3 Signal processing flowchart

Many features are extracted from cluster signatures. For each feature, the fuzzy logic has a logic sense, a criterion level, a criterion span and a criterion weight. The logic sense sets the choice between the transition 0 to 1 and the inverse. The criterion level corresponds to the center of the fuzzy transition and the span gives the transition width. The global fuzzy

$$GF = \prod_i \left(\left(F_i \cdot W_i \right) + 1 - W_i \right), \qquad (1)$$

is the product of individual fuzzy F_i values considering the corresponding weight W_i where $0 < F_i < 1$ and $0 < W_i < 1$. Table 1 gives the criterion level and scale unit of the major features.

Table 1
Cluster signature features and typical criterion levels

Features	Sense	Level	Unit
PRPD distribution matching	both	0.85	-
PRPD distribution $\Delta\theta/\Delta A$	1 to 0	75	Deg/dBmV
Form factor	0 to 1	0.15	Bin/ns
Raise lobe frequency	0 to 1	37	MHz
Time dispersion Δt	1 to 0	80	µs
RMS main lobe/ RMS noise	0 to 1	2	-
E lobe Max / E lobe Before	0 to 1	5	-
Number of half-cycle	1 to 0	6	Count
RMS cluster phase dispersion	1 to 0	40	Deg.
Inverse polarity exsistence	0 to 1	0.95	-

"PRPD distribution matching" is a correlation factor between a measured and a memorized distribution. The sense is 0 to 1 for the matching of a potentially dangerous PD. The dispersion ratio $\Delta\theta/\Delta A$ is specifically used for gap discharge identification. "Form factor" corresponds to the $\Delta f/\Delta t$ ratio estimated from a time-frequency filtered spectrogram. The time dispersion is estimated from the time signal envelope extracted with the convolutional form of the Hilbert transform [8]. "E lobe" means lobe energy integral. The "number of half-cycles" is evaluated for the time duration given by the time dispersion Δt. The existence of inverse polarity is a correlation factor between a cluster signature and the negative value of another cluster signature. A five count in the sum of cluster populations having a global fuzzy greater than 0.5 generates an alarm.

We have tested, without great success, the dispersion estimations Δf and Δt proposed by [9]. In the "raise lobe frequency", Δf is focused on the rising edge of the transient. In the "time dispersion Δt", the use of the Hilbert transform eliminates the contribution of the signal phase information.

TIME DOMAIN CLUSTERING

Time domain clustering is a maximum likelihood pattern recognition algorithm where the time signal generates its own description base. Assuming a constant normalized time signature S_n over different amplitudes, one obtains

$$X_{mn} = a_m \cdot S_{n-d_m} + n_{mn} \qquad (2)$$

the realization of the measurement "m" of a transient signature, where a_m is the realization amplitude, d_m the realization delay and n_m the additive noise. The successive measurements taken over one analog input scale are called a sequence. The a_m dynamic range is less than 10 dB for a sequence, i.e. the ratio of the clipping level on the trigger setting level. The first step clustering described here is performed for a fixed scale. The full dynamic range is obtained in a second step by merging the clusters obtained from different A/D scales. In some cases, the a_m dynamic range exceeds 30 dB. Assuming a Gaussian noise and disregarding the a_m dynamic, the $\mathbb{R}^N$ projection shows a hypersphere centered on the "i" signature

$$\mathbf{S}_i = \left\{ S_{i,1}, S_{i,2}, ..., S_{i,N} \right\} \qquad (3)$$

where the measurements

$$\mathbf{X}_m = \left\{ X_{m,1}, X_{m,2}, ..., X_{m,N} \right\} \qquad (4)$$

are close to the hypersphere boundary. For an Euclidian metric, the distance

$$D_{m,i} = \min \left\{ \sqrt{\sum_{n=1}^{N} \left(X_{m,n-d} - S_{i,n} \right)^2} \right\}_{d \in \left\{ -\frac{T}{2}, \frac{T}{2} \right\}} \qquad (5)$$

has the expected mean

$$r_i = \mathrm{E}\left(D_{m,i} \right) = \sqrt{N\,\mathrm{E}\left(n_{mn}^2 \right)} \qquad (6)$$

for $\mathbf{X}_m \in$ cluster "i" and the standard deviation

$$\sigma_i = \sqrt{\mathrm{E}\left(n_{mn}^2 \right)} \cdot \qquad (7)$$

Figure 4 illustrates in $\mathbb{R}^N$ the radius r_i and hypersphere boundary thicknesses $2\cdot\sigma_i$. The ratio of the boundary thickness on the hypersphere radius tends to 0 when $N\to\infty$. Calculated using numerous noise samples, the distance $\mathbf{X}_m-\mathbf{S}_i$ appears barely constant.

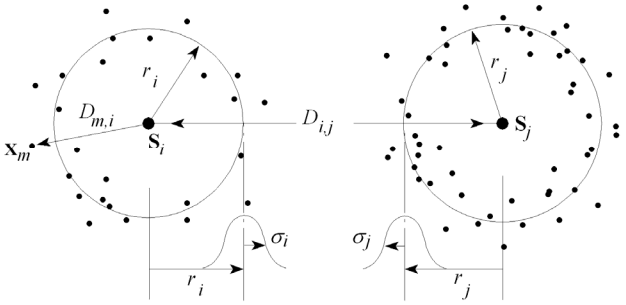

Fig. 4 Multidimensional illustration of two clusters

In $\mathbb{R}^N$, cluster probability densities appear like distributed shells with similar radius and thickness. With the presence of a significant a_m dynamic, the single point signature is replaced by a rod pointing to the axis origin. The corresponding shell is dilated along the axis of the rod. The shell thickness is increased in the rod's direction. The e use of an appropriate metric can partially overcome this shell distortion. Correlation is use instead minimum distance for the last TDC done to merge the different scales.

The merge process "segment to cluster" or "cluster to cluster" is driven by minimum distance between "segment to signature" or "signature to signature". The merge process $\mathbf{S}_i\cup\mathbf{S}_j\to\mathbf{S}_i'$ is

$$\mathbf{S}_i' = \frac{1}{P_i+P_j}\left(P_i\mathbf{S}_i + P_j\mathbf{S}_j\right) \qquad (8)$$

for the new signature calculation where P_i and P_j are the cluster populations. The overall calculation complexity tends to $O(N\times T\times M\times I)$ where N, T, M, I are respectively the numbers of time samples, the numbers of time steps tested for the time realignment, the number of segments and the number of clusters. For more details see [10].

PRPD AND PD MINING

The maximum number of captured segments for a scale is typically fixed at 100. On the first or second lower measuring scale it is common to fill up the buffer in less than a few degrees when the event rate is high. Processing the whole 360° with a continuous capture is time- and memory-consuming. The proposed PD mining optimizes the sampling of the PRPD in order to capture hidden PD clusters. The PRPD is observed through a double discretization (Fig.5): the discrete overlapped scales in amplitude and the discrete phase step mining. Best results are obtained with variable phase step PD mining (Fig.6). With variable step PD mining, the maximum phase step is 15° and the successive steps and buffer dimensions are adjusted to reach 360° with ≈200 additional segments.

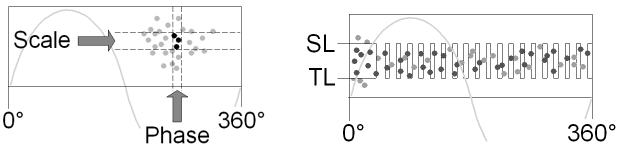

Fig. 5 Double discretization (left). Constant phase PD mining (right), saturation level (SL), trigger level(TL).

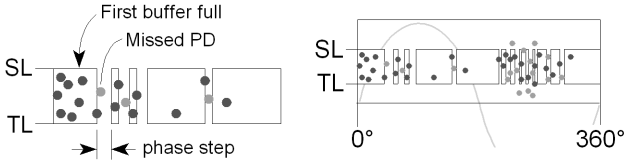

Fig. 6 Variable phase steps PD mining.

CASE STUDIES

In a vault environment, a typical sniffer measurement shows 3 to 30 clusters superimposed in the "relative phase-resolved" diagram. As illustrated in Figure 7, a large dynamic range PRPD is better illustrated with a logarithm scale. The bright green dot corresponds to a 94-segment cluster. Similar signature patterns are illustrated in dark green and opposed polarity patterns are illustrated in red.

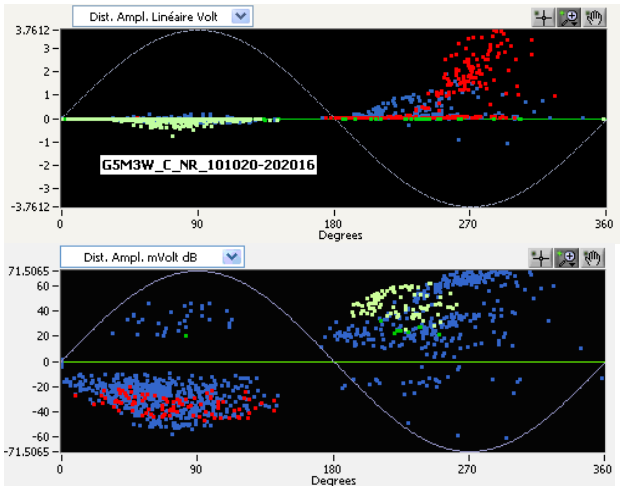

Fig. 6 PRPD diagram illustrating 1142 events, 30 clusters, in a linear scale (top) and a log scale (bottom).

Certain equipment, such as SF6 interrupters, have internal gap PDs which do not constitute a safety concern and should not raise an alarm. Gap PDs are characterized by flat PRPD distributions (Fig.7). With the help of the $\Delta\theta/\Delta A$ criterion, the sniffer discriminates between PDs originating from the latter equipment and those arising from many other possible sources. Last summer, two workers evacuated a vault after an "alarm" was signaled by the sniffer. Three hours later, the cable splice exploded in the vault. Figure 8 shows the small-amplitude PD cluster which triggered the alarm. Figure 9 illustrates two similar clusters of opposed polarities (light green and red) of PDs emitted by external

equipment in the vicinity and captured on an elbow "T" connector. Note the PD mining hatching.

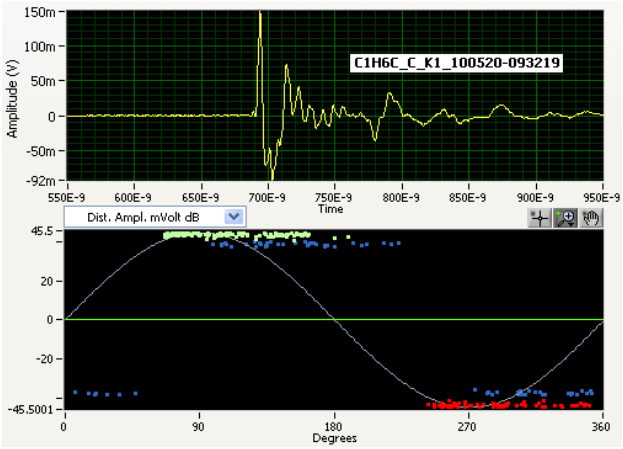

Fig. 7 Time signature and PRPD diagram of a 128 DP cluster (green) captured in the vicinity of an interrupter.

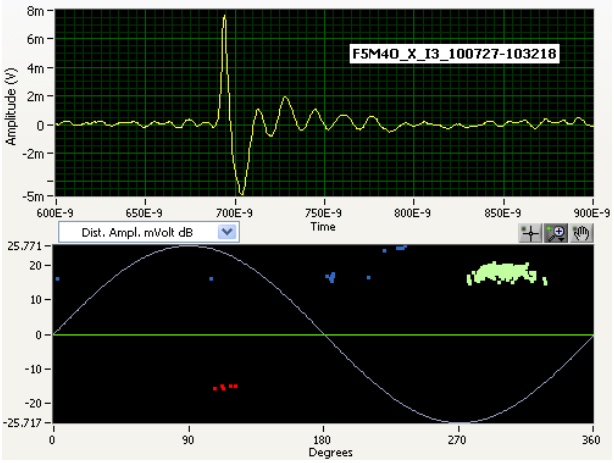

Fig. 8 Time signature and PRPD diagram of a 251 DP cluster (green) captured on a cable splice.

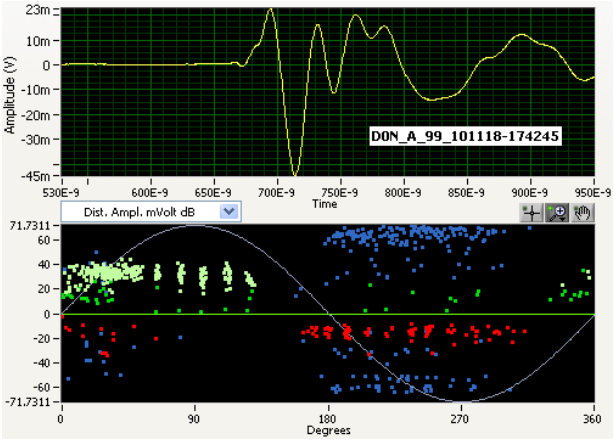

Fig. 9 Time signature and PRPD diagram of a 239 external DP cluster (green) captured with PD mining.

CONCLUSION

The sniffer has now been deployed for two years and is used with confidence by the workers. Many hundreds of measurements have been performed each week and contribute to the continuous optimization of fuzzy criteria. The external trigger through an FM notch filter is used occasionally and appears useful. The TDC preserves most of the information available from high dynamic-amplitude, large-bandwidth transient signals. With the TDC, the information is reduced to a few signatures instead of numerous measurements, the SNR signature increases with the cluster population and the post-processing time is reduced. TDC, PD mining, new cluster signature features, electronic hardware with high dynamic amplitude and a large bandwidth are the main elements of the sniffer's success.

REFERENCES

[1] D. Fournier et al., 2005, "Detection, location and interpretation of partial discharges in the underground network at Hydro-Québec," *Acts of the CIRED Conference*.

[2] M. de Nigris et al., 2002,"Cable Diagnosis based on defect location and characterization through partial discharge measurements," *CIGRE 2002*, Paper 15-109.

[3] A. Kraetge, K. Rethmeier, M. Krüger, P. Winter, 2010, "Synchronous Multi-Channel PD Measurements and the Benefits for PD Analyses," *T&D, IEEE PES*, New Orlean.

[4] A. Belkov, A. Obralic, W. Koltunowicz and R. Plath, 2010 "Advanced approach for automatic PRPD pattern recognition in monitoring of HV assets," *ISEI*, San Diego.

[5] T. Zhiguo et al., 2008,"Pulse interferences elimination and classification of on-line UHF PD signals for power transformers," *IEEE CMD 2008*, Beijing, China, 937-940, .

[6] A. Contin and S. Pastore, 2004, "An Algorithm, Based on Auto-Correlation Function Evaluation, for the Separation of Partial Discharge Signal," *IEEE International Symposium on Electrical Insulation*, Indianapolis, 19-22.

[7] T. Babnik, R.K. Aggarwal, and P.J. Moore, 2008, "Principal Component and Hierarchical Cluster Analyses as Applied to Transformer Partial Discharge Data," *IEEE Transactions on Power Delivery*, vol. 23, no. 4.

[8] F. Léonard, M. Foata, C. Rajotte, 2001, "Vibro-acoustic signature treatment process in high-voltage electromechanical switching system," *US patent 6,215,408*.

[9] A. Contin, A.Cavallini, G.C. Montanari, G.Pasini, F. Puletti, 2000, "Artificial Intelligence Methodology for Separation and Classification of Partial Discharge Signals," *Conference on Electrical Insulation and Dielectric Phenomena*, 522-526.

[10] F. Léonard, 2011, "On the use of time domain clustering in partial discharge detection, location and diagnosis," *IEEE ICASSP*, Prague, Czech Republic. Waiting for reviewer decision.